Characterization of "Mini-Nucleotides" as P2X Receptor Agonists in Rat Cardiomyocyte Cultures. An Integrated Synthetic, Biochemical, and Theoretical Study

Bilha Fischer,*[†] Revital Yefidoff,[†] Dan T. Major,[†] Irit Rutman-Halili,[‡] Valadimir Shneyvays,[‡] Tova Zinman,[‡] Kenneth A. Jacobson,[§] and Asher Shainberg[‡]

Department of Chemistry and Faculty of Life Sciences, Gonda-Goldschmied Medical Research Center, Bar-Ilan University, Ramat-Gan 52900, Israel, and NIH, NIDDK, LBC, Molecular Recognition Section, Bethesda, Maryland 20892-0810

Received February 22, 1999

The design and synthesis of "mini-nucleotides", based on a xanthine-alkyl phosphate scaffold, are described. The physiological effects of the new compounds were evaluated in rat cardiac cell culture regarding Ca^{2+} elevation and contractility. The results indicate biochemical and physiological profiles similar to those of ATP, although at higher concentrations. The biological target molecules of these "mini-nucleotides" were identified by using selective P2-R and A_1-R antagonists and P2-R subtype selective agonists. On the basis of these results and of experiments in Ca^{2+} free medium, in which $[Ca^{2+}]_i$ elevation was not observed, we concluded that interaction of the analogues is likely with P2X receptor subtypes, which causes Ca^{2+} influx. Theoretical calculations analyzing electronic effects within the series of xanthine-alkyl phosphates were performed on reduced models at quantum mechanical levels. Calculated dipole moment vectors, electrostatic potential maps, and volume parameters suggest an explanation for the activity or inactivity of the synthesized derivatives and predict a putative binding site environment for the active agonists. Xanthine-alkyl phosphate analogues proved to be selective agents for activation of P2X-R subtypes, whereas ATP activated all P2-R subtypes in cardiac cells. Therefore, these analogues may serve as prototypes of selective drugs aiming at cardiac disorders mediated through P2X receptors.

Introduction

Intracellular ATP plays a fundamental and ubiquitous role in energy metabolism, nucleic acid synthesis, pump activities, and enzyme regulation. There is also widespread evidence that extracellular adenine nucleotides exert significant biological actions on various tissues,[1] which are mediated via membrane ATP receptor (P2-R) subtypes termed P2X and P2Y. [2]

It has been shown that cardiac cells have P2 receptors that modulate transmembrane potential and cytosolic Ca^{2+} concentrations.[3] Extracellular ATP in micromolar concentrations causes Ca^{2+} elevation in cardiac cells grown in culture, which is explained as a result of production of 1,4,5-inositol triphosphate.[4] ATP is also known to cause complex changes in the heart function when infused through the circulation.[5] These changes are difficult to interpret from a mechanistic or cellular perspective because of the variety of cell types present, the complexity of the cardiac function, and the rapid degradation of ATP to adenosine. Use of neonatal rat cardiac myocyte cultures obviates many of the difficulties of the whole heart system and permits the use of the fluorescent indicators (e.g., indo-1) in intracellular Ca^{2+} measurements.

Currently, all identified P2-R agonists are compounds based on a nucleotide skeleton modified at the purine ring, sugar moiety, or the triphosphate chain.[6] Synthetic analogues circumvent some of the problems inherent in ATP, e.g., lack of enzymatic stability, relatively low affinity at P2-Rs, and lack of receptor subtype selectivity.[6] However, as nucleotides they still may potentially interact with the multitude of other ATP binding and metabolizing proteins ubiquitous in mammalian physiology.

Our goal was, therefore, to design novel selective P2-R agonists based on a "mini-nucleotide" scaffold, namely, a structure lacking a ribose moiety and having a modified purine. Further, we aimed for the evaluation of these agonists as prototypes of selective drugs for cardiac disorders mediated by P2 receptors.

In this paper we report the first synthesis of non-ATP-based P2X-R agonists, their biochemical and physiological evaluation on cultured rat cardiac cells, interpretation of the structure-activity relationship (SAR), as well as prediction of the putative binding site of these ligands based on theoretical calculations.

Results

Chemistry. Design of "Mini-Nucleotides". The guidelines for the design of new P2-R ligands, which are structurally different from ATP, were obtained by studying various protein–nucleotide complexes available in the Protein Data Bank (PDB). Assuming that binding interactions with small molecules may be of the same type in both enzymes and receptors, the structures of the complexes were probed for possible electrostatic interactions (up to 10 Å between heavy atoms), hydro-

* Address correspondence to Bilha Fischer, Department of Chemistry, Bar-Ilan University, Ramat-Gan 52900, Israel. Tel: 972-3-5138303. Fax: 972-3-5351250. E-mail: bfischer@mail.biu.ac.il.
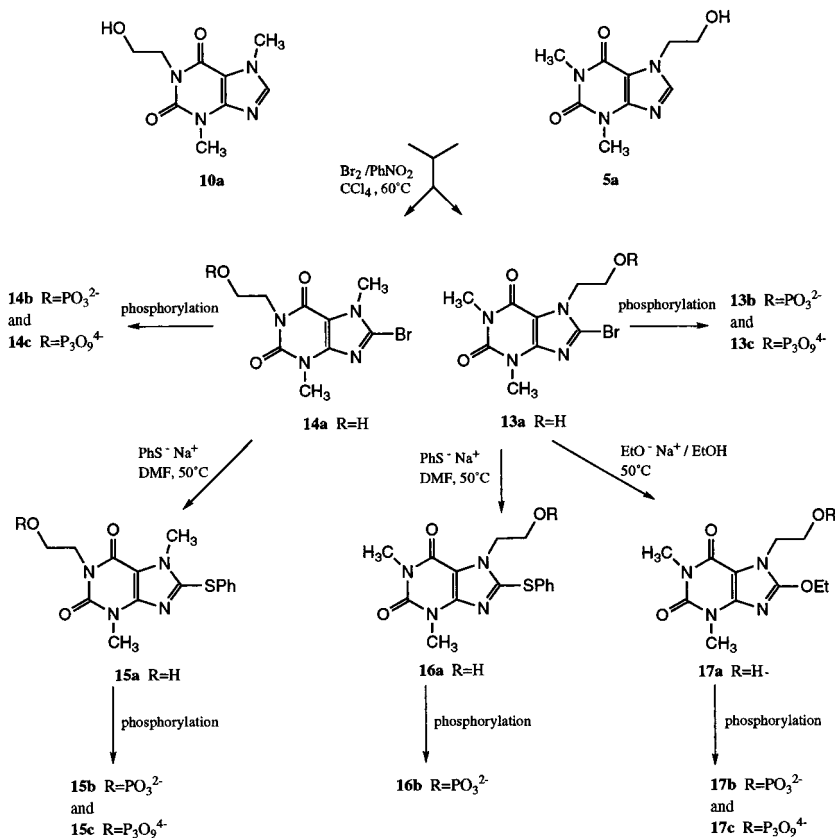† Department of Chemistry, Bar-Ilan University.
‡ Faculty of Life Sciences, Bar-Ilan University.
§ NIH.

Scheme 1. Synthesis of Xanthine Alkyl Phosphate Analogues, Compounds **6**−**7** and **11**−**12**
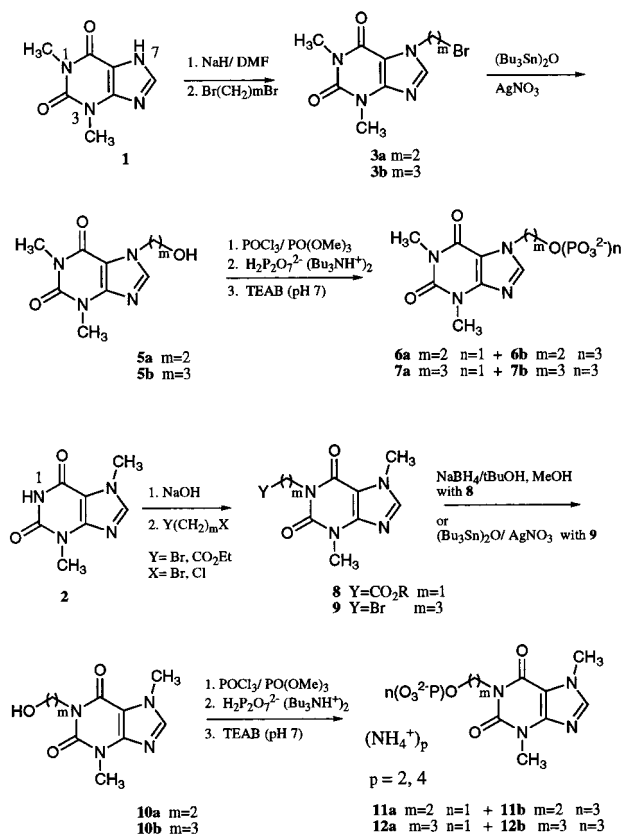
A major interaction common in all cases was the binding of the triphosphate moiety to positively charged amino acid residues (Lys or Arg) present in the binding site. Ribose 2′- and/or 3′-hydroxyls were typically hydrogen-bonded to Glu or Asp residues or to amide functions in the protein backbone. The adenine moiety was typically bound via N^6 H-bonding with Gln, Arg, or Lys or via π-stacking interactions, e.g., with Tyr.

On the basis of the PDB data, it was suggested that a new structure hypothesized to occupy a P2-R binding site might contain a heterocyclic planar skeleton (capable of forming H-bonds as well as π-stacking or hydrophobic interactions) and a negatively charged moiety tethered to it.

Recent reports have indicated that adenosine-based agonists and xanthine-based antagonists binding to the adenosine A_1 receptor share similar electrostatic properties.[7] The electrostatic features which dictate binding of both adenosine and xanthine ligands to the same site in the A_1 receptor might also hold true for the interactions of other recognition sites, namely, P2-Rs, with adenosine 5′-triphosphate and possibly with an appropriately modified xanthine.

Therefore, as a reasonable starting point for identifying new P2-R ligands, we chose xanthine derivatives (theobromine and theophylline) which share several structural and electrostatic similarities with adenine. To complete the analogy to ATP we substituted these compounds with an alkyl spacer bearing a mono- or triphosphate moiety, thus obtaining a "mini-nucleotide" structure (Schemes 1−3).

gen bonds (up to 5 Å between heavy atoms), and aromatic interactions (up to 10 Å between heavy atoms).

Synthesis of *N*-Alkyl Phosphate Theobromine and Theophylline Derivatives. Theophylline (1,3-

Scheme 2. Synthesis of 8-Substituted Xanthine-Alkyl Phosphate Analogues, Compounds **13**−**17**
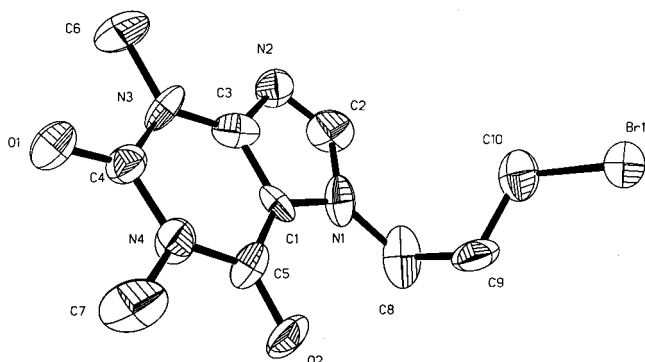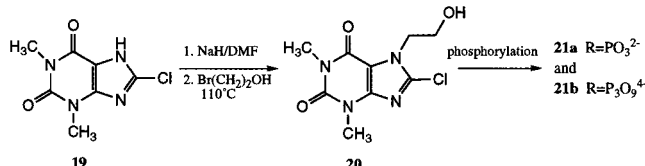
**Figure 1.** ORTEP drawing of **3b** from X-ray analysis.

Scheme 3. Synthesis of 8-Cl-7-(2-Phosphate-ethylene)-theophylline Derivatives, Compounds **21a,b**

dimethyl-xanthine), **1**, and theobromine (3,7-dimethyl-xanthine), **2**, were used as starting materials for the synthesis of a series of N-7 or N-1 alkyl phosphate derivatives (Scheme 1). The new compounds were obtained as follows: (a) isolation of dimethyl-xanthine sodium salt; (b) alkylation with an ethyl haloester or a dihaloalkane; (c) formation of a primary alcohol at the end of the side chain; (d) one-pot phosphorylation of the primary alcohol.

For SAR studies, the *N*-alkyl phosphate xanthine derivatives **6**−**7** and **11**−**12** were modified with respect to the following parameters: (1) alkyl phosphate position, namely, N-1 substitution (on theobromine) or N-7 substitution (on theophylline); (2) length of the spacer, namely, the alkyl tether linking the phosphate to the xanthine scaffold, which may consist of two or three methylenes; (3) length of the phosphate chain, which may consist of one or three phosphate residues. These variations were expected to shed light on the stereo-electronic requirements of the receptor binding site.

N-7 alkylation of theophylline, **1**, was performed by treatment with NaH/DMF followed by dibromoalkane addition at 60 °C. In addition to product **3b**, dimer **4** was isolated in 28% yield, even though the alkylating agent was present in excess. Alkylation took place selectively at N-7 as clearly shown in the X-ray crystal structure of **3b** (Figure 1).
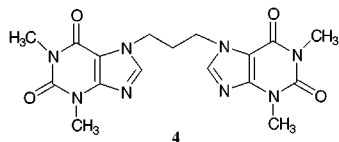
N-1 alkylation of theobromine, **2**, was carried out by NaOH addition and isolation of the dry sodium salt followed by treatment with ethyl halocarboxylate[8] in the presence of a catalytic amount of NaI or by treatment with dihaloalkane (Scheme 1). No O-alkylation products were obtained under these conditions.[9]

Hydroxyl formation at the end of the side chain was achieved either by NaBH$_4$/*t*-BuOH/MeOH reduction of

ester **8**[10] or by treatment of the bromo derivative **9** with bis(tributyltin)oxide/silver nitrate followed by hydrolysis.[11]

Finally, products **5a,b** and **10a,b** were subjected to a one-pot phosphorylation with phosphorus oxychloride[12] followed by addition of bis(tributylammonium)-pyrophosphate, to produce triphosphate derivatives **6b**, **7b**, **11b**, and **12b**. The corresponding monophosphate derivatives were isolated as side products.[12]

Synthesis of C-8 Substituted *N*-Alkyl Phosphates Xanthine Derivatives. Next, various electronic effects on the xanthine ring system that might affect binding affinity to P2-Rs were studied. The scope of the search for "mini-nucleotides" as potential P2-R ligands was therefore extended to C-8 substituted alkyl phosphate xanthines **13**−**17** and **21**. The C-8 position in **6a,b** and **11a,b** was substituted with either electron-withdrawing atoms (Cl, Br) or electron-donating groups (OEt, SPh) (Scheme 2).

Thus, 8-chloro-7-(2-monophosphate-ethylene)-theophylline and the corresponding triphosphate derivative, **21a,b**, were obtained from 8-chloro-theophylline, **19**, by treatment with NaH followed by addition of 2-bromo-ethanol and then one-pot triphosphorylation (Scheme 3). 8-Bromo derivatives were prepared from 1-(2-hydroxyethylene)-theobromine, **10a**, and 7-(2-hydroxyethylene)-theophylline, **5a**, treated with Br$_2$ in nitrobenzene/CCl$_4$ solution.[13] 8-Bromo-1-(2-hydroxyethylene)-theobromine, **14a**, and 8-bromo-7-(2-hydroxyethylene)-theophylline, **13a**, were used also as starting materials for the preparation of the corresponding 8-ethoxy and 8-thiophenyl derivatives **15**−**17** by treating the former ones with sodium ethoxide/EtOH or sodium thiophenolate/DMF, respectively (Scheme 2). Treatment of **13a** with EtONa led, in addition to **17a**, to a tricyclic product, **18** (35% yield), formed by intramolecular cyclization. To reduce the amount of side product **18**, the reaction time was shortened to 5 min. Derivatives **15a**−**17a** were finally phosphorylated as described before.
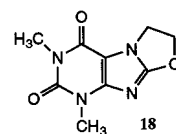
Biochemical and Physiological Evaluation. The novel derivatives were evaluated on rat cardiomyocytes as potential P2-R agonists. Their pharmacological effect was evaluated by measurements of intracellular Ca^{2+} elevation and contractility of the cells. These effects were compared with those of standard P2-R agonists (ATP, 2-MeS-ATP, and α,β-CH$_2$-ATP). In our series of experiments we explored the effect of the new compounds on the heart and characterized them as P2-R ligands. Moreover, we studied their selectivity to certain P2-R subtypes and their possible interaction with other receptors, e.g., A$_1$-R, ryanodine-R. Next, the structure−activity relationship of these ligands and their possible use as protoypes for selective drugs for treatment of cardiac disorders involving P2-Rs were analyzed.

Intracellular Ca^{2+} Elevation. To evaluate the new compounds as potential P2-R ligands, their effect on intracellular Ca^{2+} elevation was measured and com-
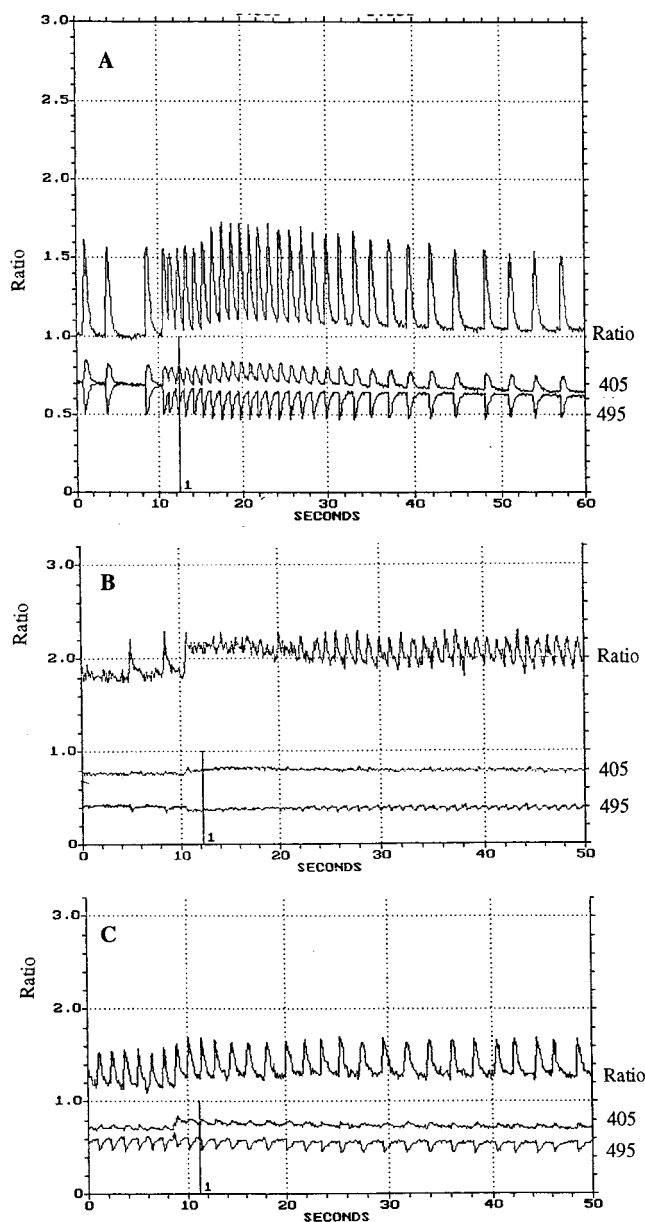
Figure 2. Effect of ATP and xanthine alkyl phosphate derivatives on intracellular Ca^{2+} concentration in cultured cardiomyocytes. Each beat was accompanied by an increase in fluorescence emission at 405 nm and a decrease in emission at 495 nm wavelength of indo-1. The ratio of 405/495 is proportional to Ca^{2+} concentration. The time of ligand addition is marked by a line (1) perpendicular to the *x*-axis. (A) Intracellular Ca^{2+} elevation associated with very rapid and short lasting Ca^{2+} transients and contractions caused by 10 μM ATP. (B) Changes caused by 100 μM **14c** were comparable to those caused by 20 μM ATP with respect to rate and magnitude of Ca^{2+} transients and contractions. (C) a moderate response was obtained with 100 μM **11a**.

pared with that of ATP. ATP at a 10 μM concentration caused intracellular Ca^{2+} elevation associated with very rapid and short lasting (20 s) Ca^{2+} transients and contractions (Figure 2A). However, upon application of a higher dose (20 μM), Ca^{2+} elevation was faster with a higher amplitude. As a result of such high concentration of intracellular Ca^{2+}, the cardiac cells became paralyzed. Later, after 30–60 s, the level of Ca^{2+} returned to the basal level and the rate of Ca^{2+} transients was reduced, as was observed for 10 μM ATP. When **14c** (100 μM) was given to the cardiac cells, results comparable to

Table 1. Effect of Xanthine Alkyl Phosphate Derivatives on Contractility and $[Ca^{2+}]_i$ Elevation[a]

compd	reductn of heart rate (%)	Ca^{2+} elevatn (nM)	compd	reductn of heart rate (%)	Ca^{2+} elevatn (nM)
		Part A			
6b	64	87 ($\pm$8)	**13b**	17	54 ($\pm$8)
6a	16	80 ($\pm$7)	**14c**	50	94 ($\pm$7)
11b	3	54 ($\pm$5)	**14b**	NA	80 ($\pm$7)
11a	10	61 ($\pm$9)	**21a**	95	49 ($\pm$5)
13c	32	37 ($\pm$7)	**21b**	28	29 ($\pm$3)
		Part B			
7b	ND	NA	**17b**	ND	NA
7a	ND	NA	**16b**	ND	NA
12b	ND	60	**16c**	ND	NA
12a	ND	NA	**15b**	ND	NA
17c	ND	NA			

[a] Cardiac cells 3–5 days in vitro were exposed to the above ligands at 100 μM concentration. Basal concentration of Ca^{2+} is 100 nM. Data of 2–3 experiments are given. $[Ca^{2+}]_i$ elevation was determined with indo-1 as previously described.[36] The rate of heart contraction was determined 1 min after drug application using motion detector system.[36] Data of representative experiments are given. NA—not active, ND—not determined.

those for 20 μM ATP were obtained with respect to rate and magnitude of Ca^{2+} transients and contractions (Figure 2B, Table 1A). Treatment of the cardiac cells with other compounds, such as **6b** and **11a** (100 μM), brought about responses similar to that of ATP (10 μM), immediately causing Ca^{2+} elevation of ca. 70 nM. A moderate response was obtained with compounds such as **14b** and **11a** (Figure 2C). A third group of agents (Table 1B) were inactive regarding Ca^{2+} elevation.

Cardiac Contractions. The effect of the new compounds on cardiomyocytes contractility was measured and compared with that of ATP. ATP at 10 μM, and the new derivatives at a 100 μM concentration, accelerated the rate of heart contractions immediately upon application. However, measurement of contractions performed 1, 5, and 30 min after application showed a reduction of heart rate (Table 1). ATP caused a 72% inhibition in cardiac contraction rate, whereas **21a** reduced the rate by 95% (from 150 to 8 bpm) after 1 min. Compound **6b** was less effective and reduced heart rate by 64% after 1 min. Compound **14c** was also effective and reduced heart rate by 50% after 1 min. Other xanthine phosphate analogues, e.g., **11b** and **13c**, were less effective in reducing contracting rate (3–32% reduction, Table 1). Compounds **11a** and **6b**, in addition to reducing heart rate, caused arrhythmia.

Characterization of the New Derivatives as P2X Receptor Ligands. To identify the P2-R subtypes, present in cardiac cells that might bind the newly synthesized ligands, standard P2Y-R and P2X-R agonists were applied and $[Ca^{2+}]_i$ was determined. Thus, when 2-methylthio-ATP (2-MeS-ATP), a potent and selective agonist for several P2Y-Rs and P2X-Rs,[6] was applied at 10 μM, a large Ca^{2+} elevation (170 nM) was observed. Ca^{2+} elevation was dose-dependent, and an increase up to 275 nM was measured upon treatment with 100 μM 2-MeS-ATP. Furthermore, at 100 μM, α,β-CH_2-ATP (a selective P2X$_1$-R and P2X$_3$-R agonist)[14] also increased calcium level (50 nM). The following order of activity was observed: 2-MeS-ATP > ATP > α,β-CH_2-ATP, indicative of the presence of P2X-R in addition to P2Y-R subtypes. Moreover, when the cells were transferred to Ca^{2+}-free PBS containing 1 mM EGTA and

Table 2. Antagonism by CPX and PPADS of the Effects of Xanthine Alkyl Phosphate Derivatives on Ca^{2+} Elevation[a]

| compd	inhibition of Ca^{2+} elevation by		compd	inhibition of Ca^{2+} elevation by	
	CPX	PPADS		CPX	PPADS
6b	−	+	**14c**	ND	+
6a	+	+	**21a**	−	ND
11b	+	−	**21b**	−	+
11a	+	+	ATP	−	+/−[b]
14b	−	+	α,β-CH₂-ATP	−	+

[a] Xanthine alkyl phosphate analogues at 100 μM concentration were added to cells incubated for 5 min with 1 μM CPX (A₁-R antagonist) or 100 μM PPADS (P2-R antagonist). Complete inhibition is designated by +. No inhibition is designated by −. ND = not determined. [b] ATP was only 60% inhibited.

treated with ATP (20 μM) or with **11b**, at 100 μM, no Ca^{2+} elevation occurred, suggesting that the rise is from calcium influx, i.e., involving P2X-R subtypes. Pyridoxal-phosphate-6-azophenyl-2′,4′-disulfonic acid tetrasodium (PPADS), which is a selective antagonist at certain P2-R subtypes,[15] was applied for distinguishing between P2 receptors and the A₁ receptor as possible sites of action of the new derivatives. Ca^{2+} elevation was completely prevented upon addition of certain analogues, e.g., **14c** and **6b** (100 μM), to cells pretreated with 100 μM PPADS cells (Table 2). However, there was still some Ca^{2+} elevation upon addition of ATP (10 μM) to PPADS (100 μM)-treated cells. The results suggest that these ligands bind to specific P2-R subtype(s), which may be blocked by PPADS, whereas ATP activates all P2-R subtypes, including those that may or may not be blocked by PPADS. To study the possible involvement of the A₁-R, an A₁-R antagonist, 8-cyclopentyl-1,3-dimethylxanthine (CPX), was added to the cardiac cells. When ATP, α,β-CH₂-ATP, or certain analogues, e.g., **6b**, were administered to CPX-treated cells, Ca^{2+} elevation was still observed, which implies that the involvement of the A₁-R is less likely. In most cases, the activity of the ligand was not blocked by CPX (Table 2). These results might imply that the new ligands bind to a P2X receptor, rather than to a P2Y-receptor or A₁-R.

Structure–Activity Relationship. The novel xanthine phosphate derivatives can be classified into two groups regarding their physiological activity (Table 1A,B). Class A, which is usually characterized by $[Ca^{2+}]_i$ elevation and reduction of contractility, consists of active xanthine-alkyl phosphate derivatives bearing hydrogen or halogen on C-8 (e.g., **6b**, **14c**, Table 1A). Class B includes inactive compounds, where the loss of activity is due to substitution of C-8 by an electron-donating group (e.g., **15c**, **17c**) or due to elongation of the alkyl spacer, tethering the phosphate to the xanthine by an additional methylene unit (e.g., **7b**, **12b**, Table 1B). In general, Class A ligands at 100 μM concentration mimicked the activity of 10 μM ATP, although with various values of $[Ca^{2+}]_i$ elevation and reduction of contractility. Class A ligands elevate $[Ca^{2+}]_i$ levels in the range of 30−95 nM. The percentage of heart rate reduction ranges from 3% to 95% (Table 1A). Within class A, there is no significant difference in activity due to the change of the position of the alkyl phosphate moiety on either N-1 or N-7, namely, between phosphorylated theobromine or theophylline derivatives (e.g., **6a** and **11a**). In class A, there was usually a small differ-

ence between triphosphate derivatives and the corresponding monophosphate derivatives with regard to $[Ca^{2+}]_i$ elevation.

SAR Interpretation and Binding Site Prediction–Theoretical Calculations. A Reduced Model for the Calculations. The structural difference between class A ligands (Table 1A) and class B ligands (Table 1B) implies that the stereoelectronic effects of the C-8 substituent may play a major role in determining activity in this set of compounds. Therefore, electronic and steric effects in the xanthine series were analyzed using molecular orbital (MO) quantum mechanical (QM) methods. The calculations were used to interpret the SAR results and to evaluate the stereoelectronic features of the ligand that dictate molecular recognition by the receptor. Moreover, the calculations' results were used for predicting a binding site for class A ligands. Theoretical analysis of the set of compounds required the use of a reduced model suitable for calculation at semiempirical and ab initio MO QM levels. SAR analysis indicates that the activity of the compounds does not depend on the position of the *N*-alkyl phosphate substitution on the xanthine, either on N-1 or N-7 (e.g., **6a** and **11a**). Furthermore, certain xanthines bearing an alkyl phosphate substitution on either N-1 or N-7, are not active at all (e.g., **15b** and **16b**). This indicates that the alkyl phosphate substitution does not solely determine activity, whereas the nature of C-8 substituents affects activity (e.g., **13b,c** and **14b,c** vs **17b,c** and **15b,c**). N-1- and N-7 alkyl phosphate xanthines possibly occupy the same conformational space in the binding pocket due to the flexibility of the alkyl phosphate group. Moreover, since the alkyl phosphate moiety has no effect on the electronic features of the xanthine, a reduced model based on caffeine (1,3,7-trimethylxanthine), **22a**, was applied. In
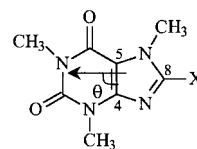
22a X = H
22b X = Br
22c X = Cl
22d X = OCH₃
22e X = SCH₃
22f X = SPh

this model, the alkyl phosphate moiety was replaced by a methyl group, and the C-8 position was substituted by either a hydrogen (**22a**), an electron-withdrawing group (**22b,c**), or an electron-donating group (**22d,e**). According to the same guidelines, ethoxy and thiophenoxy groups were replaced by methoxy and thiomethyl, respectively. Such changes make almost no difference in resonance or inductive effects. This simplified model, which bears no conformational or tautomeric complications, was used for the description of the electronic nature of the modified xanthines by calculating dipole moment vectors and electrostatic potential maps and for the description of steric effects by calculating the volume of the modified xanthines. The former helps to determine factors such as potential H-binding and complementarity of the xanthine moiety with the protein binding cavity.

Table 3. Calculated Dipole Moment Vectors for a Series of Caffeine Derivatives Using HF/3-21G* and HF/6-31G*

| | dipole moment | | | | |
| | HF/3-21G* | | HF/6-31G* | | |
compd	value (D)	angle (deg)[a]	value (D)	angle (deg)[a]	expt
caffeine	4.1518	75.13	4.2697	77.60	4.70 ± 0.05 (benzene)[b]
8-bromo-caffeine	3.0690	69.06	2.9524	73.06	
8-chloro-caffeine	2.7465	65.80	2.7877	70.42	
8-methoxy-caffeine	5.0449	105.47	5.1264	103.71	
8-thiomethyl-caffeine	4.0823	102.52	4.3010	104.85	
8-thiophenyl-caffeine	4.4109	106.90	4.8501	112.28	

[a] The dipole moment vector angle was defined as the clockwise angle between the axis from C-4 to C-5 and the dipole moment vector. [b] Reference 19.

Table 4. Minima in the Electrostatic Potential in the Vicinity of Hydrogen-Bonding Atoms at the 0.002 electron/au^3 Isodensity Surface[a]

| | $V_{min}(r)$ (kcal/mol) | | | | | |
| | HF/3-21G* | | | HF/6-31G* | | |
compd	O-2	O-6	N-9	O-2	O-6	N-9
caffeine	−55.084	−48.495	−47.929	−47.041	−41.775	−39.151
8-bromo-caffeine	−52.953	−46.472	−45.418	ND[b]	ND[b]	ND[b]
8-chloro-caffeine	−52.473	−45.896	−45.764	−44.162	−38.424	−36.138
8-methoxy-caffeine	−56.279	−50.925	−39.496	−47.824	−45.121	−31.291
8-thiomethyl-caffeine	−55.017	−50.298	−38.870	−45.822	−42.200	−30.184

[a] Wave functions were found using HF/3-21G* and HF/6-31G*. [b] Not determined as the 6-31G* basis set for Br is not included in PC Spartan 1.0.

Validation of Calculation Method. The electronic characteristics of the ligand, represented by the reduced models **22a–e**, were analyzed using MO QM calculations. The appropriate calculation method was selected by conducting first AM1[16] followed by ab initio (HF/3-21G and HF/6-31G*[17]) calculations on the reduced models and comparing the calculated geometry and dipole moment with experimental values. Thus, HF/3-21G* bond lengths and bond angles were calculated for caffeine, **22a**, and compared with the X-ray crystal structure of **3b** (because of the lack of X-ray structure for caffeine). Average absolute errors in bond lengths and bond angles were 0.015 Å and 1.1°, respectively. For the HF/6-31G* calculation, the values were 0.020 Å and 1.0°. These average absolute errors in bond lengths and bond angles are within the acceptable range, as discussed by Hehre.[18] Therefore, HF-SCF methods with small basis sets (3-21G* and 6-31G*) were considered reliable for further calculations. Indeed, the dipole moment calculated for caffeine using HF/6-31G* (0.43 D) was the closest to the experimental value, Table 3.[19] For analogues **22d,e** geometry optimizations were performed on the most stable conformer in the gas phase.

Dipole Moment. The dipole moment vector describes the charge distribution in a molecule and may thus account for electronic effects involved in molecular recognition. Therefore, dipole moment values were calculated for **22a–e** at both AM1 (results not shown) and ab initio levels (HF/3-21G* and HF/6-31G*). Table 3 describes dipole moment values and vector direction, expressed by the clockwise angle between the axis from C-4 to C-5 and the dipole moment vector. The dipole size and angle are smaller in the electron-poor derivatives (**22b,c**) than in the electron-rich derivatives (**22d,e**). This is explained in terms of known properties of the substituted groups. The derivatives bearing electron-donating groups (**22d,e**) have larger electron densities at O-6, in accordance with a possible resonance struc-ture, as indicated by a large dipole directed toward O-6 In **22b,c**, the dipole is smaller and pointing more toward O-2. These results suggest that the series of caffeine model derivatives divides to two distinct classes, based on the vector direction. Caffeine (8-H), as well as 8-Br- and 8-Cl-caffeine, form one group defined by an angle range of 70.42–77.60, whereas 8-MeO-, 8-MeS-, and 8-SPh-caffeine form a second class with an angle range of 103.1–112.28.

Molecular Electrostatic Potentials. H-binding is one of the factors dictating binding of a small molecule to a protein. Therefore, the electrostatic potential of H-bond acceptors of the xanthine scaffold, e.g., O-2, O-6, and N-9 was explored as a function of various C-8 substituents. The molecular electrostatic potential (MEP)[20] represents the first perturbation order interaction energy between a molecule and a proton. Since H-bonds are mainly electrostatic in nature,[21] the MEP may be used to model potential H-binding sites. Specifically, the minimum in the MEP, $V(r)_{min}$, is used to predict sites vulnerable to electrophilic attacks and possible H-bond acceptors.[22]

The MEP was calculated at the 0.002 electrons/au^3 electron isodensity surface,[23] as this procedure has been successfully applied to biological recognition processes.[24] The maps for **22b,c** were electron-poor and the **22d,e** maps were electron-rich relative to caffeine. All derivatives showed three clear minima in $V(r)$ in the vicinity of O-2, O-6, and N-9 (Table 4). For **22d,e** the two oxygens, O-2 and O-6, were more electronegative than in caffeine. Models **22b,c** showed less attraction for the point positive charge with O-2 and O-6. Furthermore, both electron-donating groups caused a larger decrease in the MEP value for O-6 relative to O-2, which is in accordance with a resonance structure for these electron-donating groups. A possible electronic requirement for a P2X-R agonist of this series is a dipole pointing more toward O-2, namely, an angle in the range of 70.5–77.6° (Table 4).

Table 5. Molecular Volumes within the 0.002 electron/au^3 Isodensity Surface Using HF/3-21G* and HF/6-31G*

	volume (Å^3)	
compd	HF/3-21G*	HF/6-31G*
caffeine	176.82	178.77
8-bromo-caffeine	201.17	ND^a
8-chloro-caffeine	196.14	196.44
8-methoxy-caffeine	203.44	205.23
8-thiomethyl-caffeine	219.07	219.13

^{a} Not determined as the 6-31G* basis set for Br is not included in PC Spartan 1.0.

Within the series of model compounds, N-1, N-3, and N-7 show relatively large $V(r)$ values, as is expected, since their lone pairs are delocalized. However, **22a**–**c**, exhibit lower V(r) values for N-9 (Table 4). In addition, N-9 in **22d,e** is significantly less negative, but the N-9 position seems blocked to H-bonds by the methyl group in **22d,e**. Recent studies of the H-binding capabilities of oxygen atoms covalently bound to an sp^2 hybridized atom showed that these are often considerably weaker H-acceptors than equivalent nitrogen atoms.[25] Therefore, it is likely that H-binding of the two carbonyls is not the only factor in molecular recognition of the theobromine and theophylline moieties at the receptor site and that N-9 possibly participates in H-binding with the receptor. Moreover, the low negativity of N-9 in models of the inactive derivatives (**22d,e**, Table 4) suggests that the role of N-9 as an H-acceptor could be crucial for binding to the protein.

Steric Factors. Electronic factors do not solely determine binding interactions with the protein, and steric factors, as well as the presence of hydrophobic moieties, could play a role. Table 5 presents the calculated volume for the series of caffeine derivatives. The larger volume of **22d,f** derivatives relative to caffeine and **22b,c** suggests an additional explanation to the loss for activity in those derivatives.

Discussion

A novel series of "mini-nucleotides", based on a xanthine-alkyl phosphate scaffold (Schemes 1–3), was evaluated for effects on Ca^{2+} elevation and contractility in rat cardiac cell cultures. The novel derivatives could be classified into two groups according to agonist activity or lack of activity (Table 1): Class A, generally characterized by [Ca^{2+}]$_i$ elevation and reduction of contractility, consisted of active xanthine-alkyl phosphate derivatives bearing hydrogen or halogen on C-8 (Table 1A); whereas class B included inactive compounds, the inactivity of which could be attributed to substitution of C-8 by electron-donating groups or to elongation of the alkyl spacer (Table 1B). Class A compounds exhibited a biochemical profile similar to that of ATP (although in higher concentrations), which might imply the involvement of certain P2-R subtypes. To test this hypothesis and to rule out the involvement of A$_1$-R or ryanodine-R, a series of experiments were performed.

The effect of the active agonists on [Ca^{2+}]$_i$ elevation in heart cells was tested in the presence of PPADS, a potent and subtype selective P2-R antagonist.[15] PPADS, which is effective at P2Y$_{1,2,6}$ receptor subtypes[15] as well as on P2X$_{1,2,3,7}$ subtypes,[15] was applied for distinguishing between P2 receptors and the A$_1$ receptor as possible binding proteins of the new derivatives. The fact that PPADS blocked the response to some of the potent ligands (e.g., **14c** and **6b**, Table 2), whereas ATP under the same conditions was not completely blocked, indicated that the synthetic ligands may be more specific than ATP in activating certain PPADS sensitive P2-receptor subtype(s). To determine the P2-R subtype(s) potentially involved in binding, 2-MeS-ATP, an agonist which is selective for certain P2Y-Rs and P2X-Rs,[14] was applied and caused a large Ca^{2+} elevation. Furthermore, α,β-CH$_2$-ATP (a P2X$_1$-R and P2X$_3$-R agonist[14]) also increased the calcium level. The following order of activity was observed: 2-MeS-ATP > ATP > α,β-CH$_2$-ATP, indicative of the presence of P2X$_1$-R or P2X$_3$-R, in addition to P2Y-R subtypes.[14] Moreover, when the cells were transferred to Ca^{2+}-free PBS containing 1 mM EGTA and treated with ATP or **11b**, no Ca^{2+} elevation occurred, suggesting that the ligands activated an ionic channel of P2X-R subtype rather than a P2Y receptor. Indeed, a recent report describes the localization of P2X$_1$ and P2X$_2$ receptors in rat heart,[26] in addition to P2Y$_{1,2,4,6}$-Rs.[27] P2X$_{1,3,4}$-Rs were shown to be present also in the human foetal heart together with P2Y$_{2,4,6}$-Rs.[3d]

A$_1$-R is the major adenosine receptor in the heart.[28] To exclude the possibility that the new ligands or their metabolites caused their physiological effect through the A$_1$-R, the cardiac cells were pretreated with CPX, an A$_1$-R antagonist. For most of the active new derivatives, CPX treatment did not block Ca^{2+} elevation (Table 2), thus the effect was not mediated by the A$_1$-R. However, in some cases, e.g., **6a**, the activity of the ligand was blocked by CPX, which indicates A$_1$-R activation; on the other hand, this ligand was also blocked by PPADS, which indicates P2-R activation (Table 2). This apparent contradiction might imply unselectivity of these analogues for P2-Rs.

The structures of the synthesized analogues resemble that of caffeine. The latter is known to release Ca^{2+} from the sarcoplasmic reticulum (SR) through ryanodine receptors.[29] However, it is unlikely that the novel analogues activate ryanodine receptors due to their highly charged structure, which prevents membrane permeability, and antagonism by PPADS.

SAR analysis indicates that the optimal spacer linking the phosphate to the xanthine scaffold is ethylene rather than propylene (Table 1 A,B). A P2X-R putative phosphate binding site adjacent to transmembrane helix 2 (TM2) was suggested recently.[30] It is possible that the new ligands bind to this phosphate binding site while the xanthine ring system binds to the upper part of TM2. If the linker between the phosphate and the xanthine is more than two methylenes long, it may shift the xanthine from its binding site and turn these derivatives (Table 1B) inactive.

Theoretical calculations, at the MO QM level, characterized the electronic features of the active derivatives vs the inactive ones and predicted the xanthine-phosphate binding site within the P2 receptor. We predict that next to the xanthine N-9 there is an H-bond donor amino acid residue. Furthermore, the low negativity of N-9 in models of the inactive derivatives (**22d,e**) suggests that the role of N-9 as an H-acceptor could be crucial for binding to the protein, although steric factors at the C-8 position may also account for inactivity of these compounds. The latter might imply a limited space

within the binding cavity, next to C-8. Dipole moments of models of the active derivatives, **22a**−**c**, are smaller than those of the electron-rich analogues, **22d,e**, and point more toward O-2. This might suggest a complementary positive binding site, or an H-bond donor in the vicinity of O-2. Thus, derivatives with a dipole moment pointing to O-6 may not fit the electronic demands of the binding site at this position and would likely be inactive.

In conclusion, several xanthine-alkyl phosphate analogues (e.g., **6a,b**, **14b,c**) proved to be useful selective agents for activation of P2X-R subtypes, whereas ATP activates all P2-R subtypes in cardiac cells. These novel "mini-nucleotides" are expected, therefore, to serve as prototypes for selective drugs aiming at cardiac disorders mediated through P2X receptors.

Materials and Methods

Chemistry. General. New compounds were characterized and resonances assigned by proton and carbon nuclear magnetic resonance using a Bruker AC-200, DPX-300, or DMX-600 NMR spectrometers. Tetramethylsilane was used as an internal standard while, for samples in D_2O, HOD signal was used as a reference at 4.78 ppm. Nucleotides were characterized also by ^{31}P NMR in D_2O using 85% H_3PO_4 as an external reference. Samples were treated with CHELEX-100 (BioRad, Richmond, CA) prior to spectral measurement. Xanthine derivatives were characterized on a AutoSpec-E fision VG mass spectrometer by chemical ionization MS and HRMS. Phosphorylated xanthines were desorbed from a glycerol matrix under FAB and HRFAB negative conditions using 6 kV Xe atoms. 2-Hydroxyethyl theophylline and 8-Cl-theophylline were obtained from Sigma Co. The preparation of tri-*n*-butylammonium pyrophosphate for the triphosphate synthesis as well as the preparation of TEAB (triethylammonium bicarbonate) buffer has been described.[6a] Silica gel (Merck 9385) was used for chromatography. Purification of phosphorylated xanthines was achieved on an Isco UA-6 LC system using DEAE A-25 Sephadex (HCO_3^- form) columns and a linear gradient of 0−0.4 or 0.6 M NH_4HCO_3. Peaks were detected by UV absorption at 280 nm using a UV detector. Their final purification was done on a Merck-Hitachi HPLC system using a semipreparative nucleoside/nucleotide 7U (1 × 25 cm, Alltech Associates, Inc., Deerfield, IL) and a linear gradient of acetonitrile (A):0.1 M triethylammonium acetate buffer (TEAA, pH 7.5) (B) (B:A) 90:10−30:70 (solvent system I) or 90:10−20:80 (solvent system II) in 20 min and with a flow rate of 5 mL/min. The purity of the "mini-nucleotides" described below was evaluated in two different solvent systems, solvent system I or II and solvent system III. Solvent system III was a linear gradient of 5 mM TBAP in MeOH (A): 60 mM ammonium phosphate and 5 mM TBAP in 90% water/ 10% MeOH (B) (A:B) 25:75−75:25 in 20 min with a flow rate of 1 mL/min on LiChroCART Lichrosher 60 RP-select B column (0.46 × 25 cm, Merck Co., Darmstadt, Germany). A diode array detector was used, and peaks absorbing at 274 nm were collected.

(3,7-Dimethyl-2,6-dioxo-2,3,6,7-tetrahydro-purine-1-yl) Acetic Acid Ethyl Ester (8a). A suspension of theobromine **2** (1 g, 5.56 mmol) and NaOH (0.22 g) in H_2O (15 mL) and EtOH (28 mL) was heated under reflux for 30 min to give a clear solution. The solvent was removed under high vacuum and heating to give theobromine sodium salt. A suspension of ethyl chloroacetate (3.4 g, 5 equiv) and NaI (4.16 g, 5 equiv) in dry DMF (16 mL) was stirred at room temperature for 2 h and added to a solution of theobromine sodium salt in DMF. After the mixture was stirred at 110 °C for 4.5 h, the solvent was removed under high vacuum. The solid residue was dissolved in $CHCl_3$, and the salts were filtered. The filtrate was extracted with water, dried over Na_2SO_4, and evaporated. The yellowish residue was crystallized from EtOH to give a

white solid, mp 163 °C (0.99 g, 67%).^{1}H NMR ($CDCl_3$, 200 MHz) δ: 7.54 (s, 1H, H-8), 4.76 (s, 2H, N1−CH₂), 4.23 (q, *J* = 7.14 Hz, 2H, CH₂O), 3.98 (s, 3H, N7−Me), 3.59 (s, 3H, N3−Me), 1.30 (t, *J* = 7.10 Hz, 3H, Me) ppm. ^{13}C NMR ($CDCl_3$, 200 MHz) δ: 168.37 (CO), 154.71 (C-6), 151.30 (C-2), 149.28 (C-4), 141.77 (C-8), 107.51 (C-5), 61.55 (CH₂O), 42.08 (N1−CH₂), 33.57 (N7−Me), 29.80 (N3−Me), 14.13 (Me) ppm. HRMS (DCI, CH_4): calcd for $C_{11}H_{15}N_4O_4$ (MH⁺) 267.1093, found 267.1060.

1-(2-Hydroxyethyl)-3,7-dimethyl-3,7-dihydropurine-2,6-dione (10). To a suspension of **8a** (0.12 g, 0.45 mmol) and $NaBH_4$ (0.205 g, 12 equiv) in hot *t*-BuOH (5.7 mL) at 90 °C was added slowly methanol (3.7 mL) over a 1.25 h period. The solvent was removed under vacuum, and the residue was separated on a silica gel column using a linear gradient of EtOAc:EtOH 4:1 as the eluent. The product was obtained as a white solid after crystallization from EtOH, mp 191 °C (0.057 g, 57%). ^{1}H NMR ($CDCl_3$, 200 MHz) δ: 7.53 (s, 1H, H-8), 4.30 (t, *J* = 4.83 Hz, 2H, N1−CH₂), 3.99 (s, 3H, N7−Me), 3.90 (q, *J* = 4.88 Hz, 2H, CH₂OH), 3.59 (s, 3H, N3−Me), 2.67 (t, *J* = 4.38 Hz, 1H, OH) ppm. ^{13}C NMR ($CDCl_3$, 300 MHz) δ: 155.91 (C-6), 152.38 (C-2), 149.01 (C-4), 141.83 (C-8), 107.71 (C-5), 62.04 (CH₂OH), 43.79 (N1−CH₂), 33.65 (N7−Me), 29.87 (N3−Me) ppm. HRMS (DCI, CH_4): calcd for $C_9H_{13}N_4O_3$ (MH⁺) 225.0987, found 225.0992.

General Phosphorylation Procedure. The phosphorylation procedure was adapted from Kovacs and Ötvös[12a] and Moffat.[12b] The reaction was carried out on **2** (12 mg, 0.054 mmol). Separation was performed on Sephadex DEAE A-25 column (5 cm × 1 cm) using 0−0.4 M NH_4HCO_3 linear gradient (350 mL of each). The product was obtained in 39% yield (9.6 mg) in 99% purity after further HPLC purification on a semipreprative column applying a linear gradient of TEAA: CH_3CN 80:20 to 40:60 in 20 min (3 mL/min). Rt = 4.08 min.

1-(2-Monophosphate-ethyl)-3,7-dimethyl-3,7-dihydro-purine-2,6-dione (11a) and 1-(2-Triphosphate-ethyl)-3,7-dimethyl-3,7-dihydro-purine-2,6-dione (11b). A solution of **2** (33 mg, 0.147 mmol) in dry trimethyl phosphate (0.8 mL), obtained upon heating, was cooled slowly in an ice bath under a nitrogen atmosphere. Proton sponge (47 mg) was added followed by a dropwise addition of $POCl_3$ (29.5 μL). After 20 min at 0 °C, TLC (propanol:NH_4OH:H_2O 11:2:7) indicated the formation of a polar product. TEAB (0.2 M, 7.35 mL) was added, and the ice bath was removed. After being stirred at room temperature for 0.75 h, the reaction solution was freeze-dried and separated on a Sephadex DEAE A-25 column applying a linear gradient of 0−0.2 M NH_4HCO_3 (250 mL of each). The appropriate fractions were freeze-dried 3 times sequentially. Product **11a** was obtained as a white powder (38% yield) after HPLC purification (Rt = 4.6 min (flow rate 3 mL/min, isocratic conditions TEAA:CH_3CN 50:50) and 3.58 min (in solvent system III)). Product **11b** was obtained as a white powder (35% yield, 90% pure) after HPLC purification (Rt = 7.1 min (flow rate 3 mL/min, isocratic conditions TEAA: CH_3CN 50:50) and 4.55 min (in solvent system III)). **11a:** ^{1}H NMR (D_2O, 300 MHz) δ: 7.87 (s, 1H, H-8), 4.23 (t, *J* = 5.64 Hz, 2H, N1−CH₂), 4.04 (q, *J* = 6.48, 5.65 Hz, 2H, CH₂OP), 3.93 (s, 3H, N7−Me), 3.50 (s, 3H, N3−Me) ppm. ^{31}P NMR (D_2O, 200 MHz, pH 5.0) δ: 1.16 (s) ppm. HRFAB: calcd for $C_9H_{12}N_4O_6P$ 303.0494, found 303.0500. UV: λmax 273.9 nm. **11b:** ^{1}H NMR (D_2O, 300 MHz) δ: 7.86 (s, 1H, H-8), 4.28 (t, *J* = 5.29 Hz, 2H, N1−CH₂), 4.17 (q, *J* = 6.12, 5.47 Hz, 2H, CH₂-OP), 3.94 (s, 3H, N7−Me), 3.52 (s, 3H, N3−Me) ppm. ^{31}P NMR (D_2O, 200 MHz, pH 9.5) δ: −5.45 (d), −9.99 (d), −21.54 (t) ppm. HRFAB: calcd for $C_9H_{13}N_4O_{12}P$ 461.9742, found 461.9663. UV: λmax 273.9 nm.

7-(2-Monophosphate-ethyl)-1,3-dimethyl-1,3-dihydro-purine-2,6-dione (6a) and 7-(2-Triphosphate-ethyl)-1,3-dimethyl-1,3-dihydro-purine-2,6-dione (6b). Product **6a** was obtained as a white powder (33% yield) after HPLC purification (Rt = 4.2 min (solvent system I) and 3.32 min (in solvent system III)). The product was >95% pure. **6a:** ^{1}H NMR (D_2O, 300 MHz) δ: 8.03 (s, 1H, H-8), 4.52 (t, *J* = 5.10 Hz, 2H, N7−CH₂), 4.06 (q, *J* = 6.60, 5.40 Hz, 2H, CH₂OP), 3.52 (s, 3H,

N3—Me), 3.33 (s, 3H, N1—Me) ppm. ^{31}P NMR (D$_2$O, 200 MHz, pH 6.0) δ: 3.20 (s) ppm. HRMS: calcd for C$_9$H$_{13}$N$_4$O$_6$P 304.0572, found 304.0486. UV: λmax at 273.9 nm. Product **6a** was obtained in 42% yield after HPLC purification (Rt = 3.0 min (solvent system I)). The product was >92% pure. **6b:** ^{1}H NMR (D$_2$O, 200 MHz) δ: 8.08 (s, 1H, H-8), 4.61 (t, J = 4.58 Hz, 2H, N7—CH$_2$), 4.31 (q, J = 4.84 Hz, 2H, CH$_2$OP), 3.54 (s, 3H, N3—Me), 3.35 (s, 3H, N1—Me) ppm. ^{31}P NMR (D$_2$O, 200 MHz, pH 6.5) δ: −9.81 (d), −10.79 (d), −22.52 (t) ppm. HRMS: calcd for C$_9$H$_{14}$N$_4$O$_{12}$P$_3$ 462.9821, found 462.9368. UV: λmax 273.9 nm.

1-(3-Bromo-propyl)-3,7-dimethyl-3,7-dihydro-purine-2,6-dione (9). A suspension of **2** (0.5 g, 2.78 mmol) and NaOH in water:EtOH (0.11 g of NaOH in 7.5:14 mL, respectively) was heated under reflux for 30 min to yield a clear solution. Evaporation of the solvent to dryness led to the theobromine sodium salt which was dissolved in DMF (14 mL) and 1,3-dibromopropane (5 mL, 10 equiv). The solution was heated to 140 °C for 2.5 h. The solvent was removed under high vacuum, and the residue was dissolved in diethyl ether and washed twice with water. The organic phase was dried over Na$_2$SO$_4$, and the solvent was removed. The residue was triturated with hexane and then crystallized from EtOH. Product **9** was obtained as a white solid in 23% (0.19 g), mp 142 °C. ^{1}H NMR (CDCl$_3$, 200 MHz) δ: 7.52 (s, 1H, H-8), 4.16 (t, J = 6.84 Hz, 2H, N1—CH$_2$), 3.99 (s, 3H, N7—Me), 3.58 (s, 3H, N3—Me), 3.45 (t, J = 6.90 Hz, 2H, CH$_2$Br), 2.25 (qu, J = 7.01 Hz, 2H, CH$_2$) ppm. ^{13}C NMR (CDCl$_3$, 300 MHz) δ: 155.20 (C-6), 151.47 (C-2), 148.88 (C-4), 141.58 (C-8), 107.59 (C-5), 40.27 (N1—CH$_2$), 33.63 (N7—Me), 31.34 (CH$_2$Br), 30.46 (CH$_2$), 29.73 (N3—Me) ppm. HRMS (DCI, CH$_4$): calcd for C$_{10}$H$_{13}$N$_4$O$_2$Br 300.0221, 302.0201; found 300.0183, 302.0214.

1-(3-Hydroxy-propyl)-3,7-dimethyl-3,7-dihydro-purine-2,6-dione (10b). To a clear solution of **9** (0.2 g, 0.67 mmol) in DMF (9 mL) was added AgNO$_3$ (0.22 g, 2 equiv) and bis-(tributyltin)oxide (0.74 mL, 2.2 equiv). The reaction mixture was stirred at room temperature for 5 days, and its color turned black. Water (20 mL) was added to the mixture. Silver salts were filtered, the solvent was removed under high vacuum, and the residue was separated on a silica gel column (MeOH:EtOAc 1:6). Product **10b** was obtained in 46% yield after crystallization from EtOH, mp 138—9 °C. ^{1}H NMR (CDCl$_3$, 200 MHz) δ: 7.56 (s, 1H, H-8), 4.18 (t, J = 6.15 Hz, 2H, N1—CH$_2$), 4.00 (s, 3H, N7—Me), 3.59 (s, 3H, N3—Me), 3.53 (t, J = 4.98 Hz, 2H, CH$_2$OH), 1.91 (qu, J = 5.10 Hz, 2H, CH$_2$) ppm. ^{13}C NMR (CDCl$_3$, 300 MHz) δ: 155.90 (C-6), 151.93 (C-2), 148.99 (C-4), 141.88 (C-8), 107.54 (C-5), 58.53 (CH$_2$OH), 37.80 (N1—CH$_2$), 33.67 (N7—Me), 30.83 (CH$_2$), 29.87 (N3—Me) ppm. HRMS (DCI, CH$_4$) calcd for C$_{10}$H$_{15}$N$_4$O$_3$ (MH$^+$) 239.1144, found 239.1139.

1-(3-Monophosphate-propyl)-3,7-dimethyl-3,7-dihydro-purine-2,6-dione (12a) and 1-(3-Triphosphate-propyl)-3,7-dimethyl-3,7-dihydro-purine-2,6-dione (12b). Product **12a** was obtained as a white powder (23% yield) after HPLC purification (Rt = 4.6 min (solvent system I) and 3.58 min (in solvent system III)). The product was >98% pure. **12a:** ^{1}H NMR (D$_2$O, 300 MHz) δ: 7.86 (s, 1H, H-8), 4.05 (t, J = 7.20 Hz, 2H, N1—CH$_2$), 3.92 (s, 3H, N7—Me), 3.90 (q, J = 6.60, 3.60 Hz, 2H, CH$_2$OP), 3.49 (s, 3H, N3—Me), 1.92 (qu, J = 7.00 Hz, 2H, CH$_2$) ppm. ^{31}P NMR (D$_2$O, 200 MHz, pH 6.0) δ: 1.38 (s) ppm. HRFAB: calcd for C$_{10}$H$_{14}$N$_4$O$_6$P 317.0650, found 317.0740. UV: λmax 273.9 nm. Product **12b** was obtained as a white powder (49% yield) after HPLC purification (Rt = 4.3 min (solvent system I) and 4.64 min (in solvent system III)). The product was 90% pure. **12b:** ^{1}H NMR (D$_2$O, 200 MHz) δ: 7.82 (s, 1H, H-8), 4.01 (qu, J = 7.28 Hz, 4H, N1—CH$_2$ + CH$_2$OP), 3.90 (s, 3H, N7—Me), 3.47 (s, 3H, N3—Me), 1.93 (qu, J = 7.02 Hz, 2H, CH$_2$) ppm. ^{31}P NMR (D$_2$O, 200 MHz, pH 6.5) δ: −9.26 (d), −10.26 (d), −22.40 (t) ppm. HRFAB: calcd for C$_{10}$H$_{16}$N$_4$O$_{12}$P$_3$ 476.9977, found 476.9970. UV: λmax 273.9 nm.

7-(3-Bromo-propyl)-1,3-dimethyl-3,7-dihydro-purine-2,6-dione (3). To theophylline **1** (1 g, 5.56 mmol) in dry DMF (10 mL) was added NaH (0.135 g, 1.1 equiv). The solution

turned clear within several min. 1,3-Dibromopropane (1.97 mL, 3.5 equiv) was added, and the solution was stirred at 60 °C for 2.5 h. The solvent was evaporated, and the residue was separated on a silica gel column (MeOH:EtOAC 1:6). Product **3** was obtained in 63% yield after crystallization from EtOH, mp 132 °C. ^{1}H NMR (CDCl$_3$, 200 MHz) δ: 7.65 (s, 1H, H-8), 4.47 (t, J = 6.43 Hz, 2H, N7—CH$_2$), 3.60 (s, 3H, N3—Me), 3.41 (s, 3H, N1—Me), 3.33 (t, J = 6.21 Hz, 2H, CH$_2$Br), 2.45 (qu, J = 6.29 Hz, 2H, CH$_2$) ppm. ^{13}C NMR (CDCl$_3$, 200 MHz) δ: 155.15 (C-6), 151.66 (C-2), 149.33 (C-4), 141.53 (C-8), 106.79 (C-5), 45.27 (N7—CH$_2$), 32.65 (CH$_2$Br), 29.83 (N3—Me), 29.41 (CH$_2$), 28.04 (N1—Me) ppm. HRMS (DCI, CH$_4$): calcd for C$_{10}$H$_{13}$N$_4$O$_2$Br 300.0221, 302.0201; found 300.0242, 302.0278. Side product 4: ^{1}H NMR (CDCl$_3$, 200 MHz) δ: 7.60 (s, H-8), 4.37 (t, J = 7.05 Hz, N7—CH$_2$), 3.59 (s, N3—Me), 3.39 (s, N1—Me), 2.55 (qu, J = 7.08 Hz, CH$_2$) ppm. MS (CI/NH$_3$) 401 (MH$^+$).

7-(3-Hydroxy-propyl)-1,3-dimethyl-3,7-dihydro-purine-2,6-dione (5b). Product **5b** was prepared as described for **10b** and was obtained in 46% yield after crystallization from EtOH, mp 133 °C. ^{1}H NMR (CDCl$_3$, 200 MHz) δ: 7.61 (s, 1H, H-8), 4.47 (t, J = 6.33 Hz, 2H, N7—CH$_2$), 3.60 (s, 3H, N3—Me), 3.58 (t, J = 5.73 Hz, 2H, CH$_2$OH), 3.42 (s, 3H, N1—Me), 2.07 (qu, J = 5.25 Hz, 2H, CH$_2$) ppm. ^{13}C NMR (CDCl$_3$, 600 MHz) δ: 155.78 (C-6), 151.51 (C-2), 149.05 (C-4), 141.62 (C-8), 107.22 (C-5), 58.04 (CH$_2$OH), 43.15 (N1—CH$_2$), 34.00 (CH$_2$), 29.86 (N3—Me), 28.15 (N1—Me) ppm. HRMS (DCI, CH$_4$): calcd for C$_{10}$H$_{15}$N$_4$O$_3$ (MH$^+$) 239.1144, found 239.1120.

7-(3-Monophosphate-propyl)-1,3-dimethyl-3,7-dihydro-purine-2,6-dione (7a) and 7-(3-Triphosphate-propyl)-1,3-dimethyl-3,7-dihydro-purine-2,6-dione (7b). Product **7a** was obtained in 54% yield after HPLC purification (Rt = 4.7 min (solvent system I) and 3.76 min (in solvent system III)). The product was >95% pure. **7a:** ^{1}H NMR (D$_2$O, 200 MHz) δ: 7.98 (s, 1H, H-8), 4.38 (t, J = 5.97 Hz, 2H, N7—CH$_2$), 3.73 (q, J = 4.68 Hz, 2H, CH$_2$OP), 3.48 (s, 3H, N3—Me), 3.30 (s, 3H, N1—Me), 2.08 (m, 2H, CH$_2$) ppm. ^{31}P NMR (D$_2$O, 200 MHz, pH 6.0) δ: 2.63 (s) ppm. FAB (negative): 316.99 (M). UV: λmax 273.9 nm. Product **7b** was obtained in 22% yield after HPLC purification (Rt = 4.13 min (solvent system I) and 3.19 min (in solvent system III)). The product was 93% pure. **7b:** ^{1}H NMR (D$_2$O, 300 MHz) δ: 8.06 (s, 1H, H-8), 4.45 (t, 2H, N7—CH$_2$), 3.93 (q, J = 4.76 Hz, 2H, CH$_2$OP), 3.53 (s, 3H, N3—Me), 3.34 (s, 3H, N1—Me), 2.18 (m, 2H, CH$_2$) ppm. ^{31}P NMR (D$_2$O, 200 MHz, pH 8.0) δ: −5.37 (d), −10.11 (d), −21.44 (t) ppm. HRFAB: calcd for C$_{10}$H$_{16}$N$_4$O$_{12}$P$_3$ 476.9977, found 476.9890. UV: λmax 273.9 nm.

8-Chloro-7-(2-hydroxy-ethyl)-1,3-dimethyl-3,7-dihydro-purine-2,6-dione (20). NaH (57 mg, 2.38 mmol) was added to a suspension of 8-chlorotheophylline (0.51 g, 2.38 mmol) in dry DMF (17 mL). When a clear solution was attained, 2-bromoethanol (6 mL, 6 equiv) was added. The reaction mixture was heated at 110 °C for 7 days. The solvent was removed under high vacuum, and the residue was separated on a silica gel column (EtOAc). Product **20** was obtained in 20% yield (0.11 g) after crystallization from EtOH, mp 159 °C. ^{1}H NMR (CDCl$_3$, 200 MHz) δ: 4.51 (t, J = 5.48 Hz, 2H, N7—CH$_2$), 3.99 (q, J = 5.06 Hz, 2H, CH$_2$OH), 3.55 (s, 3H, N3—Me), 3.39 (s, 3H, N1—Me), 2.74 (t, J = 5.77 Hz, 1H, OH) ppm. ^{13}C NMR (CDCl$_3$, 300 MHz) δ: 155.04 (C-6), 151.20 (C-2), 147.45 (C-4), 139.38 (C-8), 108.31 (C-5), 61.34 (CH$_2$OH), 48.41 (N7—CH$_2$), 29.93 (N3—Me), 28.16 (N1—Me) ppm. HRMS (DCI, CH$_4$): calcd for C$_9$H$_{12}$N$_4$O$_3$Cl (MH$^+$) 259.0597, found 259.0617.

8-Chloro-7-(2-monophosphate-ethyl)-1,3-dimethyl-3,7-dihydro-purine-2,6-dione (21a) and 8-Chloro-7-(2-tri-phosphate-ethyl)-1,3-dimethyl-3,7-dihydro-purine-2,6-dione (21b). Product **21a** was obtained in 28% yield after HPLC purification (Rt = 4.8 min (solvent system I) and 4.21 min (in solvent system III)). The product was >98% pure. **21a:** ^{1}H NMR (D$_2$O, 300 MHz) δ: 4.56 (t, J = 5.21 Hz, 2H, N7—CH$_2$), 4.10 (q, J = 6.14, 5.47 Hz, 2H, CH$_2$OP), 3.49 (s, 3H, N3—Me), 3.33 (s, 3H, N1—Me) ppm. ^{31}P NMR (D$_2$O, 200 MHz, pH 6.0) δ: 2.56 (s). HRFAB: calcd for C$_9$H$_{11}$N$_4$O$_6$PCl 337.0104, found 337.0060. UV: λmax 278.8 nm. Product **21b** was

obtained in 39% yield after HPLC purification (Rt = 5.1 min (solvent system I)). **21b:** ^{1}H NMR (D$_2$O, 200 MHz) δ: 4.60 (t, *J* = 3.90 Hz, 2H, N7−CH$_2$), 4.31 (q, *J* = 5.71 Hz, 2H, CH$_2$OP), 3.48 (s, 3H, N3−Me), 3.32 (s, 3H, N1−Me) ppm. ^{31}P NMR (D$_2$O, 200 MHz, pH 6.0) δ: −10.28 (d), −11.00 (d), −22.72 (t) ppm. HRFAB: calcd for C$_9$H$_{13}$N$_4$O$_{12}$P$_3$Cl 496.9431, found 496.9480. UV: λmax 278.8 nm.

8-Bromo-7-(2-hydroxy-ethyl)-1,3-dimethyl-3,7-dihydro-purine-2,6-dione (13a). Br$_2$ (0.75 mL, 1.7 equiv) in nitrobenzene (1.2 mL) was added dropwise to a suspension of 2-hydroxyethyl theophylline (1.87 g, 8.34 mmol) in nitrobenzene (8.8 mL) and CCl$_4$ (2.85 mL). The reaction solution was heated at 60 °C, with an efficient ice−water cooling, for 4.5 h. Unreacted starting material was removed by filtration. Nitrobenzene was removed from the filtrate by distillation, and the residue was separated on a silica gel column (MeOH:CHCl$_3$ 1:6). Product **14a** was obtained as a yellowish solid (0.45 g, 18%) after crystallization from EtOH, mp 172 °C. ^{1}H NMR (CDCl$_3$, 200 MHz) δ: 4.52 (t, *J* = 5.37 Hz, 2H, N7−CH$_2$), 3.98 (q, *J* = 5.28 Hz, 2H, CH$_2$OH), 3.56 (s, 3H, N3−Me), 3.39 (s, 3H, N1−Me), 2.85 (t, *J* = 5.85 Hz, 1H, OH) ppm. ^{13}C NMR (CDCl$_3$, 300 MHz) δ: 155.07 (C-6), 151.09 (C-2), 148.39 (C-4), 128.29 (C-8), 109.49 (C-5), 61.51 (CH$_2$OH), 49.36 (N7−CH$_2$), 29.95 (N3−Me), 28.20 (N1−Me) ppm. HRMS (DCI, CH$_4$): calcd for C$_9$H$_{12}$N$_4$O$_3$Br (MH$^+$) 303.0092, found 303.0090.

8-Bromo-7-(2-monophosphate-ethyl)-1,3-dimethyl-3,7-dihydro-purine-2,6-dione (13b) and 8-Bromo-7-(2-triphosphate-ethyl)-1,3-dimethyl-3,7-dihydro-purine-2,6-dione (13c). Product **13b** was obtained 53% yield after HPLC purification (Rt = 5.7 min (solvent system I) and 4.32 min (in solvent system III)). The product was >98% pure. **13b:** ^{1}H NMR (D$_2$O, 300 MHz) δ: 4.53 (t, *J* = 5.40 Hz, 2H, N7−CH$_2$), 4.31 (q, *J* = 6.30 Hz, 2H, CH$_2$OP), 3.47 (s, 3H, N3−Me), 3.31 (s, 3H, N1−Me) ppm. ^{31}P NMR (D$_2$O, 200 MHz, pH 6.5) δ: 3.16 (s) ppm. HRFAB: calcd for C$_9$H$_{11}$N$_4$O$_6$PBr 380.9599, found 380.9600. UV: λmax 280 nm. Product **13c** was obtained 37% yield after HPLC purification (Rt = 5.3 min (solvent system I) and 3.33 min (in solvent system III)). The product was >98% pure. **13c:** ^{1}H NMR (D$_2$O, 300 MHz) δ: 4.60 (t, *J* = 4.54 Hz, 2H, N7−CH$_2$), 4.30 (qu, *J* = 8.43, 4.95 Hz, 2H, CH$_2$OP), 3.48 (s, 3H, N3−Me), 3.31 (s, 3H, N1−Me) ppm. ^{31}P NMR (D$_2$O, 200 MHz, pH 5.5) δ: −10.23 (d), −11.01 (d), −22.68 (t) ppm. HRFAB: calcd for C$_9$H$_{15}$N$_4$O$_{12}$P$_3$Br 542.9082, found 542.9050. UV: λmax 280 nm.

7-(2-Hydroxy-ethyl)-1,3-dimethyl-8-phenylsulfanyl-3,7-dihydro-purine-2,6-dione (16a). To a solution of thiophenol (6 μL, 1.1 equiv) in dry DMF (10 mL) was added NaH (14 mg, 1.1 equiv), and a clear solution was attained within several min. Compound **13a** (160 mg, 0.52 mmol) in dry DMF (4 mL) was added to the thiophenolate solution. The reaction mixture was heated at 50 °C for 2 h. The solvent was removed under high vacuum, and the residue was separated on a silica gel column (MeOH:EtOAc 1:6). The product was obtained as a yellowish solid in 71% yield (0.125 mg) after crystallization from EtOH/CHCl$_3$ mp 137 °C. ^{1}H NMR (CDCl$_3$, 200 MHz) δ: 7.45−7.32 (m, 5H, Ph), 4.58 (t, *J* = 5.14 Hz, 2H, N7−CH$_2$), 3.83 (q, *J* = 5.22 Hz, 2H, CH$_2$OH), 3.53 (s, 3H, N3−Me), 3.38 (s, 3H, N1−Me), 3.00 (t, *J* = 5.92 Hz, 1H, OH) ppm. ^{13}C NMR (CDCl$_3$, 300 MHz) δ: 155.61 (C-6), 151.21 (C-2), 148.54 (C-4), 147.45 (C-8), 131.06 (C−H), 130.77 (C-ipso), 129.59 (C−H), 128.53 (C−H), 109.49 (C-5), 61.87 (CH$_2$OH), 48.60 (N7−CH$_2$), 29.97 (N3−Me), 28.18 (N1−Me) ppm. HRMS (DCI, CH$_4$): calcd for C$_{15}$H$_{17}$N$_4$O$_3$S (MH$^+$) 333.1021, found 333.1015.

7-(2-Monophosphate-ethyl)-1,3-dimethyl-8-phenylsulfanyl-3,7-dihydro-purine-2,6-dione (16b). Product **16b** was obtained in 33% yield after HPLC purification (Rt = 9.3 min (solvent system I) and 14.12 min (in solvent system III)). The product was 98% pure. **16b:** ^{1}H NMR (D$_2$O, 300 MHz) δ: 7.50−7.35 (m, 5H, Ph), 4.66 (m, 2H, N7−CH$_2$), 4.07 (m, 2H, CH$_2$OP), 3.43 (s, 3H, N3−Me), 3.33 (s, 3H, N1−Me) ppm. ^{31}P NMR (D$_2$O, 200 MHz, pH 5.5) δ: 3.63 (s). HRFAB: calcd for C$_{15}$H$_{16}$N$_4$O$_6$PS 411.0528, found 411.0630. UV: λmax 297.5 nm. Product **16c** was obtained in 44% yield after HPLC purification (Rt = 4.6 min (solvent system I) and 12.64 min (in solvent

system III)). The product was >98% pure. **16c:** ^{1}H NMR (D$_2$O, 300 MHz) δ: 7.49−7.38 (m, 5H, Ph), 4.72 (t, *J* = 4.38 Hz, 2H, N7−CH$_2$), 4.31 (qu, *J* = 7.76, 4.33 Hz, 2H, CH$_2$OP), 3.44 (s, 3H, N3−Me), 3.34 (s, 3H, N1−Me) ppm. ^{31}P NMR (D$_2$O, 200 MHz, pH 5.5) δ: −9.08 (d), −11.23 (d), −22.49 (t) ppm. HRFAB: calcd for C$_{15}$H$_{18}$N$_4$O$_{12}$P$_3$S 411.0528, found 411.0400. UV: λmax 297.5 nm.

8-Ethoxy-1-(2-monophosphate-ethyl)-1,3-dimethyl-3,7-dihydro-purine-2,6-dione (17a). To a solution of **13a** (173 mg, 0.57 mmol) in absolute EtOH (15 mL) was added sodium ethoxide solution (14 mg, in 1.4 mL EtOH). After 5 min, the solvent was evaporated and the residue was separated on a silica gel column (MeOH:EtOAc 1:6). Product **17a** was obtained as white needles in 52% (80 mg) after crystallization from EtOH/CHCl$_3$, mp 176 °C. ^{1}H NMR (CDCl$_3$, 200 MHz) δ: 4.54 (q, *J* = 7.09 Hz, 2H, CH$_2$), 4.24 (t, *J* = 5.46 Hz, 2H, N7−CH$_2$), 3.89 (t, *J* = 5.44 Hz, 2H, CH$_2$OH), 3.51 (s, 3H, N3−Me), 3.36 (s, 3H, N1−Me), 1.45 (t, *J* = 7.08 Hz, 3H, Me) ppm. ^{13}C NMR (CDCl$_3$, 300 MHz) δ: 155.88 (C-8), 155.45 (C-6), 151.47 (C-2), 146.92 (C-4), 103.53 (C-5), 67.47 (CH$_2$), 61.75 (CH$_2$OH), 45.45 (N7−CH$_2$), 29.48 (N3−Me), 27.94 (N1−Me), 14.62 (Me) ppm. HRMS (DCI, CH$_4$): calcd for C$_{11}$H$_{17}$N$_4$O$_4$ (MH$^+$) 269.1249, found 269.1233. Side product **18**: ^{1}H NMR (CDCl$_3$, 200 MHz) δ: 5.15 (t, *J* = 7.80 Hz, 2H, CH$_2$O), 4.44 (t, *J* = 7.80 Hz, 2H, N7−CH$_2$), 3.52 (s, 3H, N3−Me), 3.39 (s, 3H, N1−Me) ppm. ^{13}C NMR (CDCl$_3$, 300 MHz) δ: 154.13 (C-6), 151.66 (C-2), 162.95 (C-8), 145.12 (C-4), 102.39 (C-5), 75.14 (CH$_2$O), 43.53 (N7−CH$_2$), 29.71 (N3−Me), 27.51 (N1−Me) ppm.

8-Ethoxy-1-(2-monophosphate-ethyl)-1,3-dimethyl-3,7-dihydro-purine-2,6-dione (17b) and 8-Ethoxy-1-(2-triphosphate-ethyl)-1,3-dimethyl-3,7-dihydro-purine-2,6-dione (17c). Product **17b** was obtained in 28% yield after HPLC purification (Rt = 6.0 min (solvent system II) and 6.62 min (in solvent system III)). The product was 85% pure. **17b:** ^{1}H NMR (D$_2$O, 300 MHz) δ: 4.53 (q, *J* = 7.11 Hz, 2H, CH$_2$), 4.29 (t, *J* = 4.94 Hz, 2H, N7−CH$_2$), 4.08 (q, *J* = 6.50, 5.36 Hz, 2H, CH$_2$OP), 3.47 (s, 3H, N3−Me), 3.29 (s, 3H, N1−Me), 1.42 (t, *J* = 7.10 Hz, 3H, Me) ppm. ^{31}P NMR (D$_2$O, 200 MHz, pH 5.5) δ: 0.81 (s). HRFAB: calcd for C$_{11}$H$_{16}$N$_4$O$_7$P 347.0756, found 347.0800. UV: λmax 281.7 nm. Product **17c** was obtained in 43% yield after HPLC purification (Rt = 5.5 min (solvent system II) and 8.01 min (in solvent system III)). The product was 90% pure. **17c:** ^{1}H NMR (D$_2$O, 300 MHz) δ: 4.56 (q, *J* = 7.20 Hz, 2H, CH$_2$), 4.35 (m, 2H, N7−CH$_2$), 4.25 (m, 2H, CH$_2$OP), 3.50 (s, 3H, N3−Me), 3.32 (s, 3H, N1−Me), 1.44 (t, *J* = 7.20 Hz, 3H, Me) ppm. ^{31}P NMR (D$_2$O, 200 MHz, pH 5.5) δ: −10.30 (d), −10.99 (d), −22.72 (t) ppm. HRFAB: calcd for C$_{11}$H$_{18}$N$_4$O$_{13}$P$_3$ 507.0083, found 507.0140. UV: λmax 281.7 nm.

8-Bromo-1-(2-hydroxy-ethyl)-3,7-dimethyl-3,7-dihydro-purine-2,6-dione (14a). Product **14a** was prepared from **10a** as described for **13a** and was obtained in 17% yield after crystallization from EtOH, mp 199 °C. ^{1}H NMR (CDCl$_3$, 200 MHz) δ: 4.28 (t, *J* = 5.37 Hz, 2H, N1−CH$_2$), 3.95 (s, 3H, N7−Me), 3.88 (q, *J* = 5.14 Hz, 2H, CH$_2$OH), 3.55 (s, 3H, N3−Me), 2.56 (t, *J* = 5.53 Hz, 1H, OH) ppm. ^{13}C NMR (CDCl$_3$, 200 MHz) δ: 154.95 (C-6), 151.95 (C-2), 148.39 (C-4), 128.68 (C-8), 109.53 (C-5), 61.91 (CH$_2$OH), 43.88 (N1−CH$_2$), 34.05 (N7−Me), 29.95 (N3−Me) ppm. HRMS (DCI, CH$_4$): calcd for C$_9$H$_{12}$N$_4$O$_3$Br (MH$^+$) 303.0092, found 303.0010; calcd for C$_9$H$_{10}$N$_4$O$_2$Br (MH$^+$−H$_2$O) 284.9987, found 285.0018.

8-Bromo-1-(2-monophosphate-ethyl)-1,3-dimethyl-3,7-dihydro-purine-2,6-dione (14b) and 8-Bromo-1-(2-triphosphate-ethyl)-1,3-dimethyl-3,7-dihydro-purine-2,6-dione Tetrakis-triethylammonium salt (14c). Product **14b** was obtained in 26% yield after HPLC purification (Rt = 6.5 min (solvent system I) and 4.82 min (in solvent system III)). The product was 93% pure. **14b:** ^{1}H NMR (D$_2$O, 300 MHz) δ: 4.23 (t, *J* = 5.84 Hz, 2H, N1−CH$_2$), 4.03 (q, *J* = 6.27, 5.83 Hz, 2H, CH$_2$OP), 3.90 (s, 3H, N7−Me), 3.46 (s, 3H, N3−Me) ppm. ^{31}P NMR (D$_2$O, 200 MHz, pH 5.5) δ: 0.92 (s) ppm. HRFAB: calcd for C$_9$H$_{11}$N$_4$O$_6$PBr 380.9599, found 380.9610. UV: λmax 280.4 nm. Product **14c** was obtained in 38% yield after HPLC purification (Rt = 5.5 min (solvent system I)). **14c:** ^{1}H NMR

(D_2O, 300 MHz) δ: 4.27 (m, 2H, N1−CH_2), 4.17 (m, 2H, CH_2-OP), 3.91 (s, 3H, N7−Me), 3.48 (s, 3H, N3−Me) ppm. ^{31}P NMR (D_2O, 200 MHz, pH 9.0) δ: −5.31, −10.45, −21.92 ppm. HRFAB: calcd for $C_9H_{15}N_4O_{12}P_3Br$ 542.9082, found 542.9110. UV: λmax 280.4 nm.

1-(2-Hydroxy-ethyl)-3,7-dimethyl-8-phenylsulfanyl-3,7-dihydro-purine-2,6-dione (15a). Product **15a** was prepared from **14a** as described for **16a** and was obtained in 68% yield after crystallization from EtOH/$CHCl_3$, mp 157 °C. ^1H NMR ($CDCl_3$, 200 MHz) δ: 7.34 (br s, 5H, Ph), 4.28 (t, $J = 5.00$ Hz, 2H, N1−CH_2), 3.90 (s, 3H, N7−Me), 3.87 (t, $J = 5.02$ Hz, 2H, CH_2OH), 3.54 (s, 3H, N3−Me), ppm. ^{13}C NMR ($CDCl_3$, 300 MHz) δ: 155.44 (C-6), 152.11 (C-2), 148.39 (C-4), 147.24 (C-8), 130.73 (C−H), 130.68 (C-ipso), 129.67 (C−H), 128.40 (C−H), 109.63 (C-5), 62.10 (CH_2OH), 43.85 (N1−CH_2), 33.17 (N7−Me), 29.97 (N3−Me) ppm. HRMS (DCI, CH_4): calcd for $C_{15}H_{17}N_4O_3S$ (MH^+) 333.1021, found 303.1010.

1-(2-Monophosphate-ethyl)-3,7-dimethyl-8-phenylsulfanyl-3,7-dihydro-purine-2,6-dione Bistriethylammonium Salt (15b). Product **15b** was obtained in 28% yield after HPLC purification (Rt = 8.8 min (solvent system II)). The product was 93% pure. ^1H NMR (D_2O, 300 MHz) δ: 7.39 (br s, 5H, Ph), 4.22 (t, $J = 5.40$ Hz, 2H, N1−CH_2), 4.04 (q, $J = 6.19, 5.74$ Hz, 2H, CH_2OP), 3.92 (s, 3H, N7−Me), 3.46 (s, 3H, N3−Me) ppm. ^{31}P NMR (D_2O, 200 MHz, pH 5.5) δ: 0.99 (s) ppm. HRFAB: calcd for $C_{15}H_{16}N_4O_6PS$ 411.0528, found 411.0400. UV: λmax 300.0 nm.

Pharmacological Evaluation. Cell Culture. Rat hearts (1−2 days old) were removed under sterile conditions and washed 3 times in phosphate buffered saline (PBS) to remove excess blood cells. The hearts were minced to small fragments and then agitated gently in a solution of proteolytic enzymes, RDB (Biological Institute, Ness-Ziona, Israel), which was prepared from a fig tree extract. The RDB was diluted 1:50 in Ca^{2+} and Mg^{2+}-free PBS at 25 °C for a few cycles of 10 min each, as described previously.[31] Dulbecco's modified Eagle's medium (DMEM) containing 10% horse serum (Biological Industries, Kibbutz Beit Haemek, Israel) was added to supernatant suspensions containing dissociated cells. The mixture was centrifuged at 300g for 5 min. The supernatant phase was discarded, and the cells were suspended again. The suspension of the cells was diluted to 1.0×10^6 cells/mL, and 1.5 mL were placed in 35 mm plastic culture dishes on collagen/gelatin-coated coverglasses. The cultures were incubated in a humidified atmosphere of 5% CO_2/95% air at 37 °C. Confluent monolayers exhibiting spontaneous contractions were developed in culture within 2 days. The growth medium was replaced after 24 h and then every 3 days.

Measurement of Contractility. Culture dishes were placed into a specially designed Plexiglas chamber exposed to a 95% air/5% CO_2 atmosphere at 37 °C. The chamber was placed on the stage of an inverted phase contrast microscope (Olympus). The contractile state of the cardiomyocytes at baseline and in response to interventions was conducted using a video motion detector system, analogous to that described by Zangen and Shainberg.[32] Analogue tracing was recorded using a oscilloscope joined through a specially designed interface to an IBM computer, and kinetic data were analyzed using Microsoft Excel.

Intracellular Ca^{2+} Measurements. Intracellular free calcium concentration, $[Ca^{2+}]_i$, was estimated from indo-1 fluorescence using the ratio method described by Grynkiewicz et al.[33] The cardiac cells grown on a coverglass were transferred to a chamber on the stage of a Zeiss inverted microscope filtered with UV epifluorescence illumination. Indo-1 was excited at 355 nm, and the emitted light was then split by a dichroic mirror to two photomultipliers (Hamamatsu, Japan) with input filters at 405 and 495 nm. The fluorescence ratio of 405/495 nm, which is proportional to $[Ca^{2+}]_i$, was monitored.

Theoretical Calculations. All geometry optimizations were first performed using Gaussian 94,[34] and the AM1, HF/3-21G*, and HF/6-31G* optimized coordinates were imported into PC Spartan 1.0.[35] Using PC Spartan, single-point calculations were performed to generate the wave functions, thus enabling the display of the dipole moment vectors and the calculation and display of molecular electrostatic potential (MEP) maps. The 8-Br-caffeine HF/6-31G* MEP map was not calculated since the PC Spartan package does not include the 6-31G* basis set for Br. Calculations with Gaussian 94 were performed on an IBM RISC/6000 computer with the AIX 4 operating system.

Supporting Information Available: X-ray crystallographic data. This material is available free of charge via the Internet at http://pubs.acs.org.

References

(1) (a) Burnstock, G. Purinergic nerves. *Pharmacol. Rev.* **1972**, *24*, 509−81. (b) King, B. F.; Townsend-Nicholson, A.; Burnstock, G. Metabotropic receptors for ATP and UTP: exploring the correspondence between native and recombinant nucleotide receptors. *Trends Pharmacol. Sci.* **1998**, *19*, 506−514. (c) Chan, C. M.; Unwin, R. J.; Burnstock, G. Potential functional roles of extracellular ATP in kidney and urinary tract. *Exp. Nephrol.* **1998**, *6*, 200−207. (d) Boaeder, M. R.; Hourani, S. M. O. The regulation of vascular function by P2 receptors: multiple site and multiple receptors. *Trends Pharmacol. Sci.* **1998**, *19*, 99−107. (e) Barnard, E. A.; Simon, J.; Webb, T. E. Nucleotide receptors in the nervous system- An abundant component using diverse transduction mechanisms. *Mol. Neurobiol.* **1997**, *15*, 103−129. (f) Inoue, K. The function of ATP receptors in the hippocampus. *Pharmacol. Res.* **1998**, *38*, 323−331. (g) Abbrachio, M. P. P1 and P2 receptors in cell growth and differentiation. *Drug Dev. Res.* **1996**, *39*, 393−406.

(2) (a) Spedding, M.; Williams, M. Development in purine and pyrimidine receptors based therapeutics. *Drug Dev. Res.* **1996**, *39*, 436−441. (b) Abbracchio, M. P.; Burnstock, G. Purinoceptors: are there families of P2X and P2Y Purinoceptors? *Pharmacol. Ther.* **1994**, *64*, 445−475. (c) Barnard, E. A.; Burnstock, G.; Webb, T. E. The G-protein coupled receptors for ATP and other nucleotides: a new receptor family. *Trends Pharmacol. Sci.* **1994**, *15*, 67−70.

(3) (a) Christie, A.; Sharma, V. K.; Sheu, S. S. Mechanism of extracellular ATP-induced increase of cytosolic Ca^{2+} concentration in isolated rat ventricular myocytes. *J. Physiol* **1992**, *445*, 369−388. (b) De Young, M. B.; Scarpa, A. Extracellular ATP induces Ca^{2+} transients in cardiac myocytes which are potentiated by norepinephrine. *FEBS Lett.* **1987**, *223*, 53−58. (c) Zheng, J. S.; Christie, A.; Levi, M. N.; Scarpa, A. Ca^{2+} mobilization by extracellular ATP in rat cardiac myocytes: regulation by protein kinase C and A. *Am. J. Physiol.* **1992**, *263*, C933−C940. (d) Bogdanov, Y.; Rubino, A.; Burnstock, G. Characterisation of subtypes of the P2X and P2Y families of ATP receptors in the foetal human heart. *Life Sci.* **1998**, *62*, 697−703.

(4) Bjornsson, O. G.; Monck, J. R.; Williamson, J. R. Identification of P2Y purinoceptors associated with voltage-activated cation channels from cardiac ventricular myocytes of the rat. *J. Biochem.* **1989**, *186*, 395−404.

(5) Hohl, C. M.; Hearse, D. J. Vascular and contractile responses to extracellular ATP: studies in the isolated rat heart. *Can. J. Cardiol.* **1985**, *1*, 207−216.

(6) (a) Fischer, B.; Boyer, J. L.; Hoyle, C. H. V.; Ziganshin, A. V.; Brizzolara, A. L.; Knight, G. E.; Zimmet, J.; Burnstock, G.; Harden, T. K.; Jacobson, K. A. Identification of potent, selective P2Y-purinoceptor agonists: structure−activity relationships for 2-thioether derivatives of adenosine 5′-triphosphate. *J. Med. Chem.* **1993**, *36*, 3937. (b) Burnstock, G.; Fischer, B.; Hoyle, C. H. V.; Maillard, M.; Ziganshin, A. V.; Brizzolara, A. L.; von Isakovics, A.; Boyer, J. L.; Harden, T. K.; Jacobson, K. A. Structure activity relationship for derivatives of adenosine 5′-triphosphate as agonists at P2-purinoceptors: heterogeneity within P2X and P2Y subtypes. *Drug Dev. Res.* **1994**, *31*, 206. (c) Boyer, J. L.; O'Tuel, J. W.; Fischer, B.; Jacobson, K. A.; Harden, T. K. 2-Thioether derivatives of adenine nucleotides are exceptionally potent agonists at adenylyl cyclase-linked P2Y-purinoceptors. *Br. J. Pharmacol.* **1995**, *116*, 2611.

(7) van der Wenden, E. M.; Price, S. L.; Apaya, R. P.; Ijzerman, A. P.; Soudijn W. Relative binding orientations of adenosine A_1 receptor ligands- a test case for distributed multipole analysis in medicinal chemistry. *J. Comput. Aided Mol. Des.* **1995**, *9*, 44−54 and references therein.

(8) (a) Marzilli, L. G.; Epps, L. A.; Sorrell, T.; Kistenmacher, T. Reaction of coordinated purines. A facile, high yield synthetic route to N7-alkylated xanthines and hypoxanthines. The structure of [bis(dimethylglyoximato) (xanthinato)-(tri-*n*-butylphosphine) cobalt (III)] and the trans influence in cobalt (III) chemistry. *J. Am. Chem. Soc.* **1975**, *97*, 3351. (b) Daly, J. W.; Hide, I.; Mueller, C. E.; Shamim, M. Caffeine analogues: Structure−activity relationships at adenosine receptors. *Pharmacology* **1991**, *42*, 309−321.

(9) (a) Lister, J. H. In *Fused pyrimidines Part II: purines*; Wiley Interscience: New York, 1971. (b) Cottam, H. B.; Shih, H.; Tehrani, L. R.; Wasson, D. B.; Carson, D. Substituted xanthines, pteridinediones, and related compounds as potential antiinflammatory agents. Synthesis and biological evaluation of inhibitors of tumor necrosis factor α. *J. Med. Chem.* **1996**, *39*, 2−9.

(10) (a) Mandal, S. B.; Giri, V. S.; Pakrashi, S. C. Sodium borohydride desulfurization of thiolactams to amines. *Heterocycles*, **1988**, *27*, 11. (b) Soai, K.; Oyamada, H.; Ookawa, A. Sodium borohydride *tert*-butyl alcohol-methanol as an efficient system for the selective reduction of esters. *Synth. Commun.* **1982**, *12*, 463−467.

(11) Gingras, M.; Chan, T. H. Silver-assisted reactions of organotin oxides. A mild, neutral and anhydrous one-step conversion of primary organic halides to alcohols. *Tetrahedron Lett.* **1989**, *30*, 279−282.

(12) (a) Kovacs, T.; Otvos, L. Simple synthesis of 5-vinyl- and 5-ethenyl-2′-deoxyuridine-5′-triphosphates. *Tetrahedron Lett.* **1988**, *29*, 4525−4528. (b) Moffat, J. G. A general synthesis of nucleoside 5′-triphosphates. *Can. J. Chem.* **1964**, *42*, 599.

(13) Kopel, H. C.; Springer, R. H.; Robins, R. K.; Schneider, F. H.; Cheng, C. C. Synthesis of some 8-substituted bis(β-chloroethyl)-amino derivatives of naturally occurring *N*-methylated purines. *J. Org. Chem.* **1962**, *27*, 2173.

(14) Fischer, B. Therapeutic applications of ATP-(P2)-receptors agonists and antagonists. *Expert. Opin. Ther. Pat.* **1999**, 9, 385−399.

(15) (a) Lambrecht, G.; Ardanuy, U.; Baumert, H. G.; Bo, X.; Hoyle, C. H. V.; Nickel, P.; Pfaff, O.; Ralevic, V.; Windschief, U.; Ziganshin, A. U.; Ziyal, R.; Mutscheler, E.; Burnstock, G. Design and Pharmacological characterization of selective P2-purinoceptor antagonists. In *Perspectives in Receptor Research*; Pharmaco Chemistry Library, Giardina, D., Piergentili, S., Pigini, M., Eds.; Elsevier Science Publishers: Amsterdam, 1996; pp 337−350. (b) Boyer, J. L.; Zohn, I. E.; Jacobson, K. A.; Harden, T. K. Differential effects of P2-purinergic receptor antagonists on phospholipase C and adenylyl cyclase-coupled P2Y purinergic receptors. *Br. J. Pharmacol.* **1994**, *113*, 614−620. **(**c) Harden, T. K.; Nicholas, R. A.; Schachter, J. B.; Lazarowski, E.; Boyer, J. L. Pharmacological selectivities of molecularly defined subtypes of P2Y receptors. In *The P2 Nucleotide Receptors*; Turner, J. T., Weisman, G., Fedan, J., Eds.; The Receptors; Humana Press: Clifton, NJ, 1997; Chapter 5, pp 109−134. (d) Evans, R. J.; Surprenant, A.; North, R. A. P2X receptors. In *The P2 Nucleotide Receptors*; Turner, J. T., Weisman, G., Fedan, J., Eds.; The receptors; Humana Press: Clifton, NJ, 1997; Chapter 2, pp 43−61.

(16) Dewar, M. J. S.; Zoebisch, E. G.; Healy, E. F.; Stewart, J. J. P. AM1: A new general purpose quantum mechanical molecular model. *J. Am. Chem. Soc.* **1985**, *107*, 3902−3909.

(17) (a) Binkley, J. S.; Pople, J. A.; Hehre, W. J. Self-consistent molecular orbital methods. 21. Small split-valence basis sets for first-row elements. *J. Am. Chem. Soc.* **1980**, *102*, 939−947. (b) Gordon, M. S.; Binkley, J. S.; Pople, J. A.; Pietro, W. J.; Hehre, W. J. Self-consistent molecular orbital methods. 22. Small split-valence basis sets for second-row elements. *J. Am. Chem. Soc.*

1982, *104*, 2797−2803. (c) Pietro, W. J.; Francl, M. M.; Hehre, W. J.; DeFrees, D. J.; Pople, J. A.; Binkley, J. S. Self-consistent molecular orbital methods. 24. Supplemented small split-valence basis sets for second-row elements. *J. Am. Chem. Soc.* **1982**, *104*, 5039−5048.

(18) Hehre, W. J.; Radom, L.; Schleyer, P. V. R.; Pople, J. A. *Ab Initio molecular orbital theory*; Wiley: New York, 1986; Chapter 6.

(19) Weiler-Feilchenfeld, H.; Bergmann, E. D. The dipole moments of some purine and pyrimidine derivatives. *Israel J. Chem.* **1968**, *6*, 823−826.

(20) (a) Naray-Szabo, G.; Ferenczy, G. G. Molecular Electrostatics. *Chem. Rev.* **1995**, *95*, 829−847. (b) Doucet, J.-P.; Weber, J. *Computer-Aided Molecular Design: Theory and Applications*; Academic Press Inc.: San Diego, CA, 1996; Chapter 10.

(21) Pauling, L. *Proc. Natl. Acad. Sci. U.S.A.* **1928**, *14*, 359.

(22) Politzer, P., Murray, J. S., Lipkowitz, K. B., Boyd, D. B., Eds. *Molecular electrostatic potentials and chemical reactivity. Reviews in Computational Chemistry*; VCH: New York 1991: Vol. 2, Chapter 7, pp 273−312.

(23) Kahn, S. D.; Pau, C. F.; Hehre, W. J. Models for chemical reactivity: Mapping of intermolecular potentials onto electron density surfaces. *Int. J. Quantum Chem., Quantum Chem. Symp.* **1988**, *22*, 575−591.

(24) Sjoberg, P.; Murray, J. S.; Brinck, T.; Evans, P.; Politzer, P. The use of the electrostatic potential at the molecular surface in recognition interactions: dibenzo-p-dioxins and related Systems. *J. Mol. Graphics* **1990**, *8*, 81−85.

(25) Nobeli, I.; Price, S. L.; Lommerse, J. P. M.; Taylor, R. Hydrogen bonding properties of oxygen and nitrogen acceptors in aromatic heterocycles. *J. Comput. Chem.* **1997**, *18*, 2060−2074.

(26) Hansen, M. A.; Balcar, V. J.; Barden, J. A.; Bennett, M. R. Localisation of P2X subtypes in heart, artery and bladder. *Drug Dev. Res.* (Special issue, 6th International Symposium on Adenosine and Adenine Nucleotides.) **1998**, *43*, 5.

(27) Webb, T. E.; Boluyt, M. O.; Barnard, E. A. Molecular biology of P2Y purinoceptors: Expression in rat heart. *J. Auton. Pharmacol.* **1996**, *16*, 303−307.

(28) Shryock, J. C.; Belardinelli, L. Adenosine and adenosine receptors in the cardiovascular system: Biochemistry, physiology and pharmacology. *Am. J. Cardiol.* **1997**, *79*, 2−10.

(29) Hasenfuss G. Alterations of calcium-regulatory proteins in heart failure. *Cardiovasc. Res.* **1998**, *37*, 279−289.

(30) Hansen, M. A.; Barden, J. A.; Balcar, V. J.; Keay, K. A.; Bennett, M. R. Structural motif and characteristics of the extracellular domain of P2X receptors. *Biochem. Biophys. Res. Commun.* **1997**, *236*, 670−675.

(31) El-Ani, D.; Jacobson, K. A.; Shainberg, A. Regulation of A_1 adenosine receptors by amiodarone and electrical stimulation in rat myocardial cells in vitro. *Biochem. Pharmacol.* **1997**, *54*, 583−587.

(32) Zangen, A.; Shainberg, A. Thiamine deficiency in cardiac cells in culture. *Biochem. Pharmacol.* **1997**, *54*, 575−582.

(33) Grynkiewicz, G.; Poenie, M.; Tsien, R. Y. A new generation of Ca^{2+} indicators with greatly improved fluorescence properties. *J. Biol. Chem.* **1985**, *260*, 3440−3450.

(34) Gaussian 94, Gaussian Inc.; Pittsburgh, PA.

(35) PC Spartan 1.0, Wavefunction Inc., Irvine, CA.

(36) Manoach, M.; Varon, D.; Shainberg, A.; Zinman, T.; Isaack, A.; Halili-Rutman, I.; Kaplan D.; Tribulova N. The protective effect of class III antiarrhythmic agents against calcium overload in cultured myocytes. *Life Sci.* **1997**, *61*, PL 227−234.